Thermal Science and Engineering Progress 52 (2024) 102678

Contents lists available at ScienceDirect

Thermal Science and Engineering Progress

journal homepage: www.elsevier.com/locate/tsep

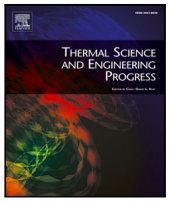

Sensitivity to heat and mass transfer correlations of the model for an evaporative condenser

M. Giovannini, M. Lorenzini *

Department of Industrial Engineering, DIN, University of Bologna, Via Fontanelle 40, Forli, I-47121, Italy

ARTICLE INFO

Keywords:
Evaporative condenser
Evaporative cooling
Refrigeration equipment
Convective heat and mass transfer coefficients

ABSTRACT

Evaporative condensers have established themselves in refrigeration plants for food process and storage owing to the combination of air and water cooling, with an overall reduction in energy (pumping) and fluid (water) consumption. Given the steep rise of electricity prices, the need to develop conduction strategies at the plant level which are less energy-intensive has driven the need for models to carry out simulations of the new strategies without actually impacting normal plant operations. This paper describes the development of a distributed-parameter model of an evaporative condenser with fill-pack, based on Merkel's pioneering works on evaporative cooling. Several correlations are available for the heat and mass transfer coefficients, but none that satisfies the operating conditions of the case at hand, yet they are the most critical set of parameters for the model, therefore a sensitivity study has been carried out, to ascertain which combinations of transport coefficients out of a total of 288 would yield a total cooling power closest to the value declared by the manufacturer for a real-life evaporative condenser under rating conditions. This work demonstrates the applicability of the correlations examined, and also twenty of the examined combinations allow the model to reach a good agreement with the reference data (within ±5%). Further, the distributed-parameter structure of the model allows highlighting the reasons for good or bad performance of the correlations by determining the spatial distribution in the cooling coil and fill-pack of quantities such as moist air enthalpy and water temperature. The model and methodologies are a little cost-intensive in terms of computational time and can be applied to the study and design of any similar piece of equipment.

1. Introduction

Evaporative condensers have found extensive use in refrigeration plants for food processing and storage. The increasing popularity they have enjoyed in the last forty years is largely due to the overall economic benefits deriving from their combination of air-cooling and water-cooling processes in one piece of equipment. Operating costs are lower in comparison with traditional condensers due to lower pumping and fan power demand owing to a reduction in the amount of water and air that circulates. The most prominent feature of evaporative condensers, however, is that they can be designed for a lower condensation temperature than single-fluid units, which in turn allows lower power consumption and lower pressure ratio designs for the compressor [1–3]. As a consequence, the heat transfer surface and the refrigerant charge in the circuit can be reduced too.

Water consumption in the condenser is moderate and can be estimated to amount to 0.4 kg per 1000 kJ of energy transferred as heat, in the case evaporation is the only means of heat removal. During summertime up to 80% of the thermal energy removed may be due to evaporation. The main disadvantages of evaporative condensers are related to fouling issues, as scale tends to form rather quickly on the outside of the tubes, and sometimes cleaning the inside of the ducts may be problematic, [4,5].

In this type of condenser the heat is transferred from the refrigerant through tube walls to a thin film of water, which is sprayed over the outer surface of the tubes, and then to air, mainly due to partial evaporation of water. Air is circulated through fans, which either blow it over the tube bundle or suck it, depending on their placement. According to the design of the evaporative condenser, air can be in co-flow, counter-flow or even cross-flow with the falling water film.

The warm water falling from the condenser coil can be collected in a sump and circulated back to the sprinklers, or, prior to collection, it can flow through a piece of heat transfer equipment, called fill-pack, where it is cooled by a stream of ambient air.

One configuration for an evaporative condenser is shown in Fig. 1. The fans at the top suck air from outside and circulate it through the unit; the airflow is split into two main streams; the first in co-flow with

* Corresponding author.
E-mail address: marco.lorenzini@unibo.it (M. Lorenzini).

https://doi.org/10.1016/j.tsep.2024.102678
Received 22 February 2024; Received in revised form 2 May 2024; Accepted 3 June 2024
Available online 5 June 2024

Nomenclature

a_{fp}	$m^2\,m^{-3}$	Air–water interface area to volume of fill pack ratio
A	m^2	Area
B	m^{-3}	Empirical constant
c	$kJ\,kg^{-1}\,K$	Specific heat capacity
D	$m^2\,s^{-1}$	Mass diffusivity
d	m	Diameter
g	$m\,s^{-2}$	Acceleration of gravity
h	$kJ\,kg^{-1}$	Specific enthalpy
Le	–	Lewis number
$\dot{m}$	$kg\,s^{-1}$	Mass flow rate
m	–	Empirical constant
n	–	Empirical constant
P	m	Tube pitch
Pr	–	Prandtl number
$\dot{Q}$	kW	Thermal power
Re	–	Reynolds number
T	°C	Temperature
V	$m\,s^{-1}$	Velocity
U	$W\,m^{-2}\,K$	Overall heat transfer coefficient
z	m	Cartesian axis direction

Greek symbols

α	$W\,m^{-2}\,K$	Convective heat transfer coefficient
β	$kg\,m^{-2}\,K$	Convective mass transfer coefficient
λ	$W\,m^{-1}\,K$	Thermal conductivity
Γ	$kg\,m^{-1}\,K$	Mass flow rate for unit length
ϕ	–	Relative humidity
μ	$N\,s\,m^{-2}$	Viscosity
ρ	$kg\,m^{-3}$	Density

Subscripts

a	Air
db	Dry bulb
c	Condensate
f	Front
fp	Fill-pack
l	Saturated liquid
lv	Liquid-to-vapour
i	Inner
m	Average
o	Outer
p	Constant pressure
r	Refrigerant
s	Saturation
sw	Saturation at water temperature
v	Saturated vapour
vol	Volumetric
w	Water
wb	Wet bulb

the falling water, crosses the condenser coil, the other, in cross-flow with the falling water blows through the fill-pack. The splitting ratio of the airflow is determined by the manufacturer at the design stage. The fill-pack consists of a modular structure in polymeric material (e.g. PVC) forming meandering channels, where heat transfer between falling water and ambient air occurs. This allows the water temperature in the sump to drop below that of the water falling from the tube bundle with positive impacts on the performance related to a reduction of the condensing temperature,[7].

Several transport phenomena occur in the evaporative condensers, and this, together with the practical significance of their knowledge for technical applications, has been the motivation for a large body of scientific investigation over the years.

Among the earliest studies on evaporation, the contributions of Merkel [8] and Poppe and Rogener [9] must be mentioned, as they influenced most of the later literature relevant to evaporative condensers: their models will be discussed further in the paper. Baker and Shyrock [10] presented a succinct application of Merkel's model to the calculation of heat transfer in evaporative heat exchangers. The doctoral thesis of Dreyer [11] outlines some methods of calculation of the heat transfer in evaporative condensers starting from Poppe's model to obtain the simpler formulation suggested by Merkel and also

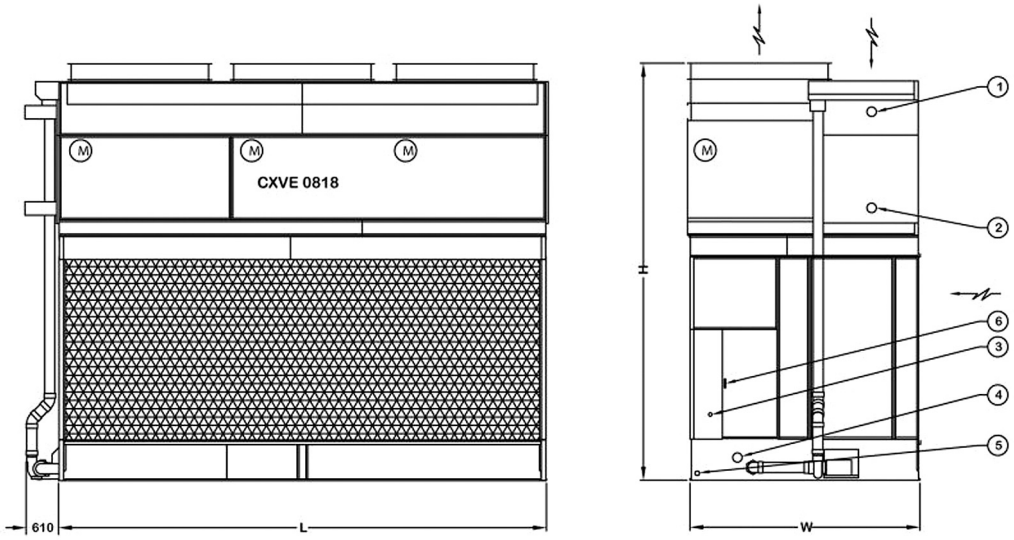

Fig. 1. Evaporative condenser with fill-pack, from BAC website. The model examined in this work is the CXVE 466-1218-45L, with the overall dimensions: $L = 5.480$ m, $W = 3.607$ m and $H = 5.349$ m [6].

offers a hint for a lumped parameter model. Dreyer also developed a code to solve the systems of differential equations involved in the two distributed-parameter models deriving from Poppe's and Merkel's approaches, with various examples of layout and working conditions. The same work lists several correlations to compute the convective heat and mass transfer coefficients, which, however, are limited to the case of air and water in counter-flow. Several types of evaporative condensers are considered, which differ for the flow direction of the fluids, layout, presence or lack of a fill-pack. The algorithms used for the calculations in [11] are explained in deeper detail in [12] where the different modes of computation according to the layout and geometry of the tubes are discussed.

Zalewski [13] proposed a one-dimensional approach to solve the equations describing heat transfer in an evaporative condenser. Poppe's model is integrated along the direction of the flows of water and air, with some assumptions on the symmetry of the process in the control volumes. The same distributed parameter approach is adopted also in [14].

Halàsz [15] offers a general if rather involved, method to compute evaporative heat transfer for different configurations and two or three fluids partaking in the process.

Hasan and Sirén [16] applied Merkel's model to the computation of evaporative heat transfer in closed wet cooling towers for HVAC applications, using a distributed parameter approach; the same subject was further expanded in [17], with simplified analytical models employed in conjunction with CFD simulations.

An extensive analysis of air-cooled heat exchangers and cooling towers is included in Kröger [18], which considers both Merkel's and Poppe's approaches with several practical applications. Heat transfer and pressure drop in the heat exchanger equipment are discussed, with a wide selection of applicable correlations suggested, also for mass transfer in the liquid film around the coil's tubes. In a further work, [19], Kloppers and Kröger discuss the effect of the Lewis factor (which had already been related to the Lewis number in [11]) on the performance of the heat exchanger for different layouts of cooling towers.

Qureshi and Zubar [20] realized a distributed parameter model of a counterflow evaporative condenser, and investigated the effect of fouling on the thermal performances; moreover he evaluates the effect of atmospheric pressure.

Facao and Oliveira, [21], compared the experimental data for an indirect contact cooling tower with the results of CFD simulations for heat and mass transfer, discussing the possibility of employing computer simulations to obtain mass transfer correlations.

In 2010 Yilmaz [22] proposed an integral analytical approach to obtain the performance of wet cooling towers, expanding on the work of Dreyer [11]. The results are compared with the well-known logarithmic mean enthalpy difference (LMED) and corrected LMED methods, reaching a good agreement.

Zheng and his co-workers [23] carried out an extensive experimental campaign on a closed wet cooling tower with air and recirculating water in counter-flow: they compared the experimental data with those predicted by a mathematical model of the evaporative cooler based on Merkel's assumptions. They also proposed two novel correlations for the heat and mass transfer coefficients. Also, the behaviour of the evaporative cooler under saturated air conditions was investigated in greater detail by the same group employing a model based on Poppe's analysis [24].

Hernández-Calderón et al. [25] proposed a more efficient way to solve the system of differential equations resulting from Poppe's formulation of the evaporative heat exchange in a counterflow wet cooling tower; the orthogonal collocation technique appears as accurate as the integration with the Dormand–Prince method, which belongs to Runge–Kutta ODE solvers family, but requires less CPU time.

Ortiz-del-Castillo et al. [26] proposed an advanced technique to solve Poppe's model for evaporation, based on the power-series method; this approach exhibited large savings in computational time while maintaining a good accuracy.

Du Plessis and Owen [27] developed a model of the evaporative heat transfer occurring in a smooth-tube bundle of a hybrid (dry/wet) dephlegmator (HDWD). The results were compared with the experimental data obtained by an *ad-hoc* counter-flow cooling tower test facility at Stellenbosch University. Assuming a unitary Lewis factor, they adopted Merkel's formulation; the resulting three differential equation system was solved by the means of a fourth-order Runge–Kutta method. As to the choice of the correlation for transport coefficients, Mizushina's was chosen for round tubes and Zheng's for oval ones.

Bhatkar [28] demonstrated a model evaporative condenser for HVAC applications which does not change the relative humidity significantly.

Recently, in [29], a distributed parameter model of an evaporative condenser according to the approach of Zalewsky [13] was developed and evaluated with a boundary value problem solver in Matlab; it was also validated and data-driven tuned with real-operating data. The

literature survey highlights how the modelling of evaporative coolers, wet cooling towers and air-cooled condensers is still a lively area of research, with modelling issues which span several areas of transport phenomena and thermodynamics and are also linked to the degree of detail required by the application. The literature survey did not evidence the existence of correlations for the co-flow of water and air, a significant issue since several realizations of evaporative condensers work in this way.

This paper investigates the use of a simplified model (Merkel's) to simulate the behaviour of an evaporative condenser with fill-pack, with a view to embedding it into a larger, mostly lumped-parameter type model, of a refrigeration plant for food (fruit and vegetables) storage located in northern Italy. The application requires that the model be little cost-intensive in terms of computational time while being physically sound so as to capture the physical behaviour of this piece of heat transfer equipment. The choice fell therefore upon a distributed-parameter model, focussing on the best choice of correlations for heat and mass transfer for the case investigated. The latter was mandated by the aforementioned lack of literature on the convective heat and mass transfer coefficients for air and water in co-flow. The results obtained are validated against the nominal cooling power declared by the manufacturer (BAC Condensers, Baltimore, USA) for a model of the evaporative condenser (BAC-CXVE) under given operating, steady-state conditions.

2. Mathematical model

According to Mansour [30], evaporative heat transfer can be modelled using to three different approaches: numerical, analytical and lumped/simplified. The first category exclusively comprises full computational thermo-fluid dynamical models, whereas simplified models usually start by dividing the system into smaller domains which are treated with a lumped-parameter approach. The choice of the model for the evaporative condenser was dictated by the final use of the model itself, i.e. the simulation of the behaviour of a refrigeration plant for fruit and vegetable storage [3]. This ruled out a full CFD model, which would be computationally too intensive and difficult to integrate into a larger framework, leaving lumped-parameter and distributed-parameter models as candidates (the issue is discussed by Kröger in [18]).

A lumped-parameter model would be a computationally more attractive choice, as quantities are at most time-dependent only, and the model becomes algebraic for steady-state conditions. Unfortunately, especially when a fill-pack is present, the underlying assumption required to use a lumped parameter formulation, i.e. that the temperature of water throughout the heat exchanger packs remains constant, is not verified in practice. This leaves no other choice but to adopt a distributed-parameter model, that is, a model whose quantities depend not only on time but also on some spatial coordinate, which is determined by the physical process that the model attempts to describe. It will also be demonstrated that a distributed description can give extra insight into the physical phenomena occurring in the system.

Several approaches found in literature have been considered, all dealing with three fluids: two (air and water) interact directly, whereas the third (the refrigerant) undergoes condensation and is separated from the others by the pipe wall. The governing equations obtained can be applied to co-flow counterflow and cross-flow arrangements, which dictate how the governing differential equations are integrated.

2.1. Poppe's model and Merkel's simplified form

An in-depth analysis of the behaviour of fluids in an air-cooled heat exchanger was proposed by Poppe, [9], whose model is applicable to cooling of a process fluid, be it with or without phase change. The model was developed for steady-state conditions, but can readily be extended to transient problems since it is based on energy and mass balances over control volumes.

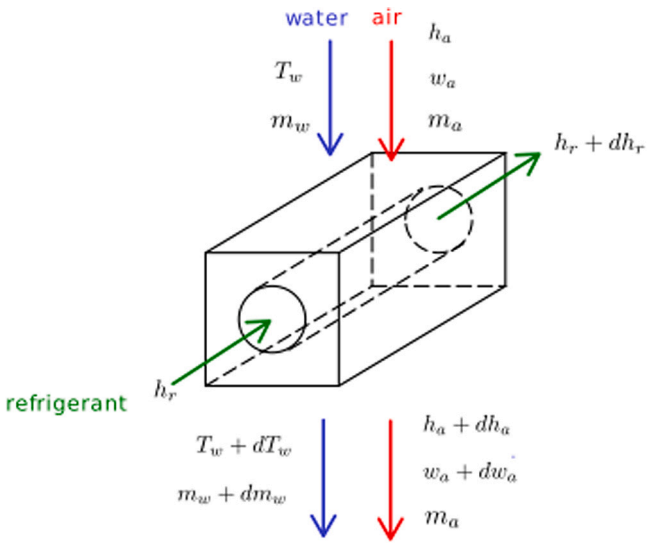

Fig. 2. Control volume for the mass and energy balances.

The underlying assumptions for the model are:

(a) negligible radiation heat transfer;
(b) uniform distribution of recirculated water, both over the coil and the fill-pack, if present;
(c) uniform temperature in the water film, owing to its small thickness (water temperature varies along the tube) ;
(d) the area of the heat/mass transfer surface between water film and moist air equals that of the outer pipe wall;
(e) contributions to heat transfer by end-elements of the coil are negligible;
(f) the enthalpy increase in the water due to the circulation pump is neglected.

In the paper, the model is applied in co-flow mode to a generic control volume. In order to reduce the number of equations to be solved, further simplifying assumptions are made, which leads to the original formulation by Merkel, [8]. These are:

(g) variations in the mass flow rate of water through the coil due to evaporation of the liquid film are neglected;
(h) the heat transfer rate during the evaporative process is comparable to the mass transfer rate (which corresponds to a Lewis number close to unity, $Le \approx 1$).

Under the above assumptions and concerning the control volume shown in Fig. 2, the governing equations used to model the refrigerant coil are listed below:

$$dh_a = \frac{\beta_t}{\dot{m}_a}(h_{a,sw} - h_a)dA_o \tag{1}$$

$$dT_w = \frac{1}{\dot{m} \cdot c_{p,w}}(\dot{m}dh_a + \dot{m}_r dh_r) \tag{2}$$

$$dh_r = \frac{U}{\dot{m}_r}(T_r - T_w)dA_o \tag{3}$$

for moist air enthalpy, water temperature, and refrigerant enthalpy respectively. When the refrigerant is superheated, one further equation is added:

$$dT_r = \frac{1}{c_{p,r}}dh_r \tag{4}$$

The pressure drop for the refrigerant flowing inside the coil is considered negligible and all thermophysical and thermodynamic properties needed in the computations are obtained from data fits of tables generated through the *CoolProp* open-source package [31].

The overall heat transfer coefficient, U, consists of three contributions, accounting for convective heat transfer in the refrigerant and in the water film and conductive heat transfer in the pipe:

$$U = \left(\frac{1}{\alpha_r}\left(\frac{d_o}{d_i}\right) + \frac{d_o}{2\lambda}\ln\left(\frac{d_o}{d_i}\right) + \frac{1}{\alpha_w}\right)^{-1} \tag{5}$$

In the fill-pack, direct contact heat transfer between the warmer water dripping from the refrigerant coil and ambient air results in a further decrease in the temperature of the liquid, which is collected in the sump below. Only two fluids are involved in the process, water and ambient air, which enter into direct contact in corrugated plastic (PVC) pads packed together to form meandering channels, so as to offer larger specific contact areas per unit volume of the fill-pack.

Applying Merkel's model to the fill-pack the governing equations become:

$$dh_a = \frac{\beta_f}{\dot{m}_a}(h_{a,sw} - h_a)dA_{fp} \tag{6}$$

$$dT_w = \frac{1}{\dot{m}\cdot c_{p,w}}\dot{m}_a dh_a \tag{7}$$

Dreyer [11], obtained the relationship between the heat transfer area A_{fp} and the front area of the fill-pack A_f through the ratio of the interface area between water droplets and air to the volume of the fill-pack a_{fp}, so that:

$$dA_{fp} = a_{fp}A_f dz \tag{8}$$

2.2. Numerical solution

The mathematical model of evaporative heat transfer over the tube bundle is represented by the system of Eqs. (1)–(3), with the addition of Eq. (4) when the refrigerant is still superheated. For the fill-pack, Eqs. (6) and (7) are needed. The equations employed are quite straightforward and can be integrated numerically using one of the several methods available. Here a fixed-step, forward Euler method was chosen, because of two reasons. The first is dictated by the physical layout of the tube bundle and by the actual path of each fluid stream: the path of the refrigerant within the tube bundle is divided into several elements of equal length, each of which resembles that in Fig. 2, where input and output fluxes of each quantity are clearly defined. Since integration progresses in the flow direction of the refrigerant, all input quantities to the $n+1$ element are known from the integration of the previous n elements. The same approach is adopted for the fill-pack, where only water and air are present. The second reason for the choice of the integration scheme is its fast computation and the fact that the main source of inaccuracy in the results is represented by the correct estimation of the transport coefficients for heat and mass transfer, as will be discussed below.

The integration path for the numerical solution of the models is shown in Fig. 3 both for the tube bundle and fill-pack. The numerical integration follows the refrigerant path in the condensing coil and the water path in the fill-pack.

The refrigeration plant, which operates with R717 (ammonia), is equipped with a liquid trap downstream of the evaporative condenser; because of this, the refrigerant mass flow rate through the tube bundle is determined by the actual heat transfer in the condenser; also, the discharge line arrangement causes the refrigerant conditions at the exit of the condenser to be those of saturated or slightly subcooled (1 − 2 K) liquid. This requires Eqs. (1)–(3) to be solved iteratively to obtain the actual mass flow rate.

3. Choice of the transport coefficients

As previously mentioned, the key issue for the model is the correct choice of transport coefficients that best replicate the performance of the actual evaporative condenser. For the condensation coil, this means choosing the convective heat transfer coefficient for the refrigerant during cooling and condensation, α_r, that for convection between the outer tube and the water film around it, α_w, and the convective mass transfer coefficient between the water film and moist air, β_t. For the fill-pack, consistently with Merkel's assumptions, only the convective mass transfer, β_f, and a ratio of the interface area between water droplets and air to the volume of the fill pack, a_{fp}, which is a specific property of the materials and particular geometry adopted by the manufactures.

The convective heat transfer coefficient in the water film around the tubes and the mass transfer coefficient between the water film on the tube and air are tightly connected and strongly related to the closed circuit evaporative cooling system; so in previous works, they were investigated together. In the following, the correlations applied for the calculation of these coefficients are briefly reviewed, based on the works of Kröger [18] and Du Plessis and Owen [27]. Heat and mass transfer occur in the fill pack too, but the determination of the mass transfer coefficient is quite different and depends strongly on the geometry of the fill-pack itself. One further issue is related to the relative arrangements of the flows of water and air in the correlations available in the open literature, where the two streams are either in crossflow or counterflow, whilst in the evaporative condenser investigated these are in co-flow, which poses the question, whether they yield correct heat and mass transport coefficients.

3.1. Transport coefficients in the tube bundle

Parker and Treybald [32] suggested an empirical correlation to compute the heat transfer coefficient for the water film covering the pipes. Their results were obtained investigating a bundle of smooth pipes with an outer diameter of 19 mm and a staggered pitch equal to twice the diameter.

$$\alpha_w = 704(1.3936 + 0,02214T_{wm})\left(\frac{\Gamma_m}{d_o}\right)^{\frac{1}{3}} \tag{9}$$

The correlation is applicable within the following bonds: $15 < T_{wm} < 70$ (°C), $1.4 < \frac{\Gamma_m}{d_o} < 3$ (kg m^{-2} s^{-1}), $Re_{wm} \simeq 5000$. For the mass transfer coefficient, the same Authors recommend:

$$\beta_t = 0.04935\left(\frac{m_a}{A_c}\right)^{0.905} \tag{10}$$

Within the range: $0.68 < \left(\frac{m_a}{A_c}\right) < 5$ (kg m^{-2} s^{-1}).

Mizushina [33] investigated staggered smooth tube banks with an outer diameter between 19 mm and 40 mm and a pitch of twice the outer diameter ($P = 2d_o$).

$$\alpha_w = 2102.9\left(\frac{\Gamma_m}{d_o}\right)^{\frac{1}{3}} \tag{11}$$

The range of applicability of Eq. (11) is defined by: $0.2 < \frac{\Gamma_m}{d_o} < 5.5$ (kg m^{-2} s^{-1}), $1500 < Re_{wm} < 8000$. For mass transfer,

$$\beta_t = 5.5439\times10^{-8}Re_{am}^{0.9}Re_{wm}^{0.15}d_o^{-1.6} \tag{12}$$

Which is valid for: $1.0\times10^3 < Re_{am} < 1.4\times10^4$, $50 < Re_{wm} < 240$.

Nitsu [34] studied staggered smooth tube banks with 16 mm outer diameter with a triangular arrangement such that $\frac{P_l}{d_o} = 2.38$ and $\frac{P_t}{d_o} = 2.34$ and obtained the following correlation:

$$\alpha_w = 990\left(\frac{\Gamma_m}{d_o}\right)^{0.46} \qquad (\mathrm{W\,m^{-2}\,K^{-1}}) \tag{13}$$

With $0.5 < \frac{\Gamma_m}{d_o} < 3.2$ kg m^{-2} s^{-1}, whilst for mass transfer

$$\beta_t = 0.076\left(\frac{m_{am}}{A_c}\right)^{0.8} \tag{14}$$

which was obtained for $1.5 < \left(\frac{m_a}{A_c}\right) < 5$ (kg m^{-2} s^{-1}).

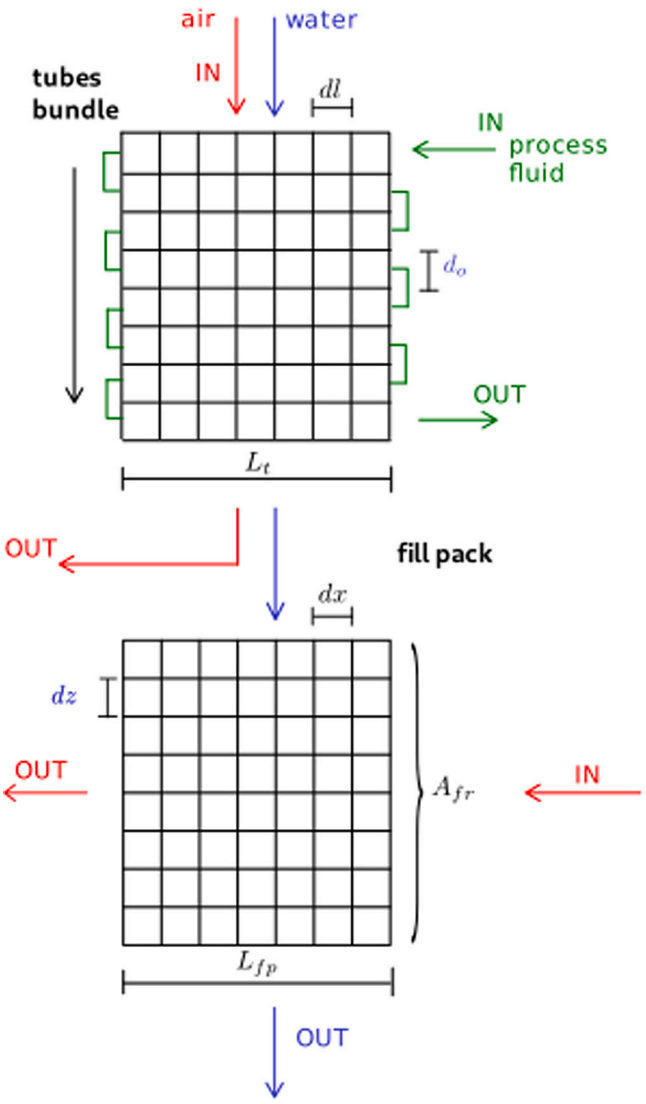

Fig. 3. Integration path for the numerical solution of the model in the tubes bundle and the fill pack.

Leidenfrost and Korenic [35] experimentally determined a correlation for staggered tube banks with a 15.9 mm outer diameter and triangular pattern defined by $\frac{P_l}{d_o} = 2.4$ and $\frac{P_t}{d_o} = 2$.

$$\alpha_w = 2064\left(\frac{\Gamma_m}{d_o}\right)^{0.252} \tag{15}$$

The range of applicability of these equations is given by $2 < \frac{\Gamma_m}{d_o} < 5.6$ (kg m^{-2} s^{-1}).

Erens and Dryer, [36] proposed a correlation for tube banks in cross-flow with external tube diameter $d_o = 38.1$ mm which yields

$$\alpha_w = 2843\left(\frac{\Gamma_m}{d_o}\right)^{0.384} \tag{16}$$

obtained for the range $0.038889 < \Gamma_m < 0.180556$ (kg m^{-1}s^{-1}). The corresponding mass transfer coefficient was determined as

$$\beta_t = 5.5749 \times 10^{-5}\, \mathrm{Re}_{am}^{0.64}\, Re_{wm}^{0.2} \tag{17}$$

The range of applicability of the correlation is $2.5 \times 10^3 < Re_{am} < 13.5 \times 10^3, 230 < Re_{wm} < 1100$.

Hasan and Siren [17] obtained another correlation for the mass transfer coefficient in evaporative cooling, through an experimental campaign with staggered tubes with $d_o = 10$ mm and longitudinal pitch $P_l = 20$ mm and traversal pitch $P_t = 60$ mm.

$$\beta_t = 0.065\left(\frac{\dot{m}_a}{A_c}\right)^{0.773} \tag{18}$$

In the range $0.96 < \left(\frac{m_a}{A_c}\right) < 2.76$ (kg m^{-2} s^{-1}).

Recently, Zheng et al. [23] carried out tests on an experimental apparatus consisting of an oval tube bundle, with the major axis of the tube 31.8 mm, and minor axis 21.6 mm, and 8 rows, in a staggered pattern with a transversal pitch of 44 mm and a longitudinal pitch of 64 mm. For the convective heat transfer coefficient in the water film, the correlation suggested is:

$$\alpha_w = 350.3(1 + 0.0169T_w)\left(\frac{\dot{m}_a}{A_c}\right)^{0.59}\left(\frac{\Gamma}{d_o}\right)^{\frac{1}{3}} \tag{19}$$

Which was obtained for the range of parameters $1.2 < \frac{\Gamma_m}{d_o} < 3.176$ (kg m^{-2} s^{-1}), $2.57 < \left(\frac{\dot{m}_a}{A_c}\right) < 4.94$ (kg m^{-2} s^{-1}), $11 < T_{wm} < 28$ (°C) with $A_c = W - N_t \frac{d_o}{2} L$.

For the mass transfer between water and air was suggested:

$$\beta_t = 0.034\left(\frac{\dot{m}_a}{A_c}\right)^{0.977} \tag{20}$$

The range of applicability is defined by $2.57 < \left(\frac{\dot{m}_a}{A_c}\right) < 4.94$ (kg m^{-2} s^{-1}).

In most cases the heat transfer coefficient is related to the water mass flowrate through a power law; Parker and Treybald, [32], and Zheng et al. [23], also pointed out a linear dependence on the mean water film temperature; also, Zheng et al. [23], consider the contribution of the air mass flow rate.

The mass transfer coefficient, conversely, is strongly related to the air mass flow rate. Mizushina, [33], and Erens and Dreyer, [36], quantified this dependence by the means of the Reynolds number for the airflow, and also considered the influence of the water flow, again through the corresponding Reynolds number.

3.2. In-tube condensation heat transfer coefficient for ammonia

The condensation heat transfer coefficient for the refrigerant inside the tubes also plays a pivotal role in the whole performance of the mathematical model, as it contributes to the overall heat transfer coefficient between the refrigerant inside and the water film around the tube, Eq. (5). Starting from the measurements by Komandiwirya et al. [37], Park and Hrnjak [38] inferred that the heat transfer rate from condensing ammonia is independent of the vapour quality for mass fluxes lower than 80 $\mathrm{kg\,m^{-2}\,s^{-1}}$. They also demonstrated that the flow patterns of the condensing ammonia, directly depending on the mass fluxes, is strictly related to the dominant heat transfer mechanism, either forced or free convective condensation; for each mechanism, they suggested the most suitable correlation for the heat transfer coefficient. In the case in point, the mass fluxes always remain below 80 $\mathrm{kg\,m^{-2}\,s^{-1}}$, so, following the recommendations in [38], the Chato correlation which describes the free convection occurring in stratified wavy flow would be the first choice

$$\alpha_r = 0.728 K_c \left[\frac{g\rho_l(\rho_l - \rho_v)\lambda_l^3 h_{lv}}{\mu_l (T_s - T_{wall}) d_i} \right] \tag{21}$$

To use Eq. (21) the inner wall's surface temperature, T_{wall} must be known; in the present study this data was neither available nor measurable, therefore another correlation, also discussed Park and Hrnjak [38] and presented in more detail by Kröger [18], which was developed by Shah, [39], was used:

$$Nu = \frac{\alpha_r d_i}{\lambda_r} = 0.023 Re^{0.8} Pr^{0.4} \left(0.55 + \frac{2.09}{p_r^{0.38}} \right) \tag{22}$$

where p_r is the reduced pressure, i.e. the ratio between the saturation pressure and the critical pressure: $p_r = \frac{p_v}{p_{cr}}$.

Park and Hrnjak, [38], however, observed that all the heat transfer correlations examined tend to overestimate the heat transfer from condensing ammonia, up to 300%.

Since ammonia enters the condenser as superheated vapour and exits as slightly subcooled liquid, a correlation for single-phase heat transfer is also required. The choice fell on the well-established Dittus-Boelter correlation, [18].

$$Nu = \frac{\alpha_r d_i}{\lambda_r} = 0.0265 Re^{0.8} Pr^{0.3} \tag{23}$$

3.3. Fill pack analysis: interface area and air–water mass transfer coefficient

The fill pack consist of a series of corrugated plastic (PVC) pads laid side by side to form channels through which the airflow crosses the water falling from the condenser tubes and gliding over the pad surfaces. The mass transfer coefficient through this element is a function of the geometry and the material of the pads and is often determined experimentally by the manufacturers themselves, who keep the value proprietary. In general, it is possible to define a volumetric mass transfer coefficient describing the overall transport properties of the fill pack, [40]. The volumetric mass transfer coefficient is often expressed by a correlation in the form:

$$\beta_{vol} = B \dot{m}_a{}^m \dot{m}_w{}^n \qquad (\mathrm{kg\,m^{-3}\,s^{-1}}) \tag{24}$$

where B, m and n are empirical coefficients available to the manufactures.

According to Dreyer, [11], in this study fill pack operation is described by Eq. (6) where the interface area between the water and the air is calculated with Eq. (8); again, as suggested by Dreyer, [11], the interface area coefficient is chosen as $a_f = 250\ \mathrm{m^2/m^3}$. On the other hand, the evaluation of the mass transfer coefficient β_f can be carried out employing the same correlations as for the coil, considering a similar evaporation process from a falling water film. The feasibility of this assumption is discussed in detail in the 'Results' section.

4. Test methodology

The many correlations listed above make it clear that the open literature offers a wide range of choices to obtain both convective heat and mass transfer coefficients in the liquid film, yet it is not known how these perform when applied to conditions which may lie, if slightly, outside the bounds for which they were obtained, nor whether correlations for both α_w and β by the same research group should be used together when available, as suggested both by Finlay and Grant [41] and by Dreyer [11].

To investigate the matter, the correlations above were used to calculate the corresponding convective coefficients (both for heat and mass transfer) for the cooling coil and the fill pack of an evaporative condenser. Owing to the lack of knowledge of the exact geometry and mass transfer performance of the fill-pack, a range of plausible values for β_f was also tested, thus leading to a total of 288 different combinations.

The two systems of differential equations, Eqs. (1)–(3) and (6)–(7) respectively, are then solved along a one-dimensional path, as per Fig. 3, to yield the temperature of the refrigerant over the coil, the enthalpy of moist air and the water temperature distributions over the cooling coil and in the fill-pack. Other quantities are also computed, namely the refrigerant mass flowrate, its enthalpy at the coil exit, the heat transfer from the coil to water and air, and the total thermal power from the refrigerant to ambient. The latter piece of information is the one needed to fit the evaporative condenser into a larger, mostly lumped-parameter model describing the refrigeration plant in its entirety. Yet, a distributed-parameter description of the condenser has been preferred for the reasons already mentioned above. Discretization of the equations has been carried out using a fixed-step, forward Euler method, implemented in a code written in Python which integrates the equations sequentially, in a way which must be consistent with the fluid flows of the actual process. It was therefore chosen to integrate along the direction of the flow of air and water. The direction of the refrigerant is perpendicular, yet its winding path is bound downwards, which makes the fluid's inlet conditions known for each element, with its outlet conditions resulting from integration fed as input to the neighbouring elements.

Computations are carried out at values of relative humidity $\phi = 46\%$, dry bulb temperature $T_{db} = 37\,^\circ\mathrm{C}$, wet bulb temperature $T_{wb} = 27.2\,^\circ\mathrm{C}$, condensation temperature $T_c = 35\,^\circ\mathrm{C}$, which for the process fluid employed (R717, ammonia) corresponds to a condensation pressure $p_c = 13.5\,\mathrm{bar}$. Under these operating conditions, the manufacturer declares for the evaporative condenser a cooling capacity of $\dot{Q}_0 = 1610\,\mathrm{kW}$.

5. Results and discussion

5.1. Grid independence verification

The code was initially checked to ensure that results were independent of the number of elements which compose the computational domain. To this purpose, some cases among all the possible combinations of correlations were picked and simulations were run progressively increasing the number of elements constituting the distributed-parameter

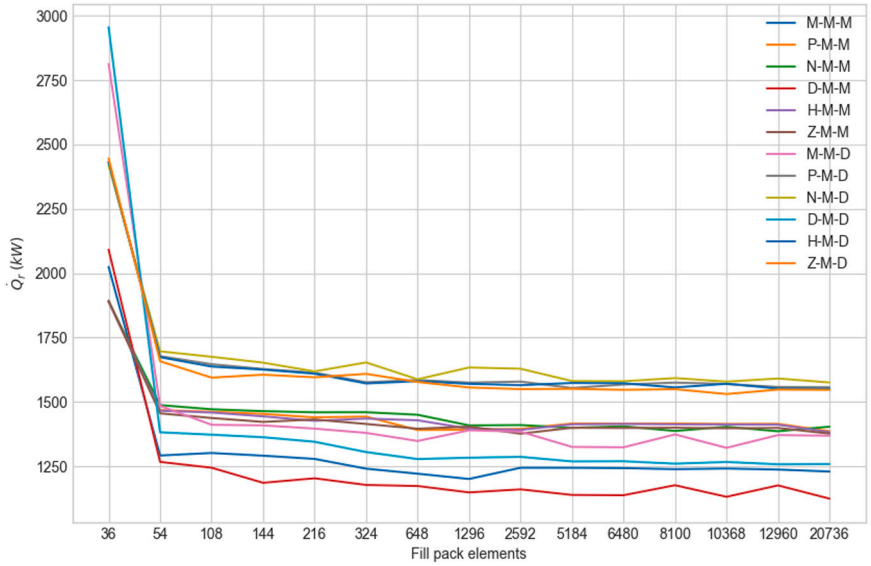

Fig. 4. Total heat transfer from the refrigerant $\dot{Q}_r$ versus number of elements; correlations of: Dreyer, [11], D, Hasan, [17], H, Mizushina, [33], M, Nitsu, [34], N, Parker, [32], P, and Zheng, [23], Z.

model. The results are plotted in Fig. 4, which shows the total heat transfer from the refrigerant as a function of the number of elements constituting the model. Each curve corresponds to a different combination of the correlations employed for the transport coefficients arranged in the order: convective mass transfer in the coil, convective mass transfer in the fill-pack, and convective heat transfer in the coil. Initials indicate the correlations chosen (D for Dreyer, H for Hasan, M for Mizushina, *N* for Nitsu, P for Parker and Z for Zheng). Based on the results of the tests and other considerations concerning stability issues, a number of 5184 elements was chosen. The total time for computations of the results and production of the associated plots for the entire range of combinations on a two-core laptop was below two hours, with CPU time for a single set of coefficients without a plot was approximately 3 s. The code yields several plots of the computed quantities, which will be described in the following. Fig. 5 shows the typical temperature distribution obtained for the refrigerant within the cooling coil, in particular, the combination of transport coefficients is Dreyer and Nitsu for heat and mass transfer in the cooling coil and Zheng for mass transfer in the fill-pack.

5.2. Local evaluation of the process variables

As already mentioned, for heat transfer between refrigerant and tube walls the Shah and Dittus-Boelter correlations, Eqs. (22) and (23), were used for all cases. With reference to Fig. 5, ammonia enters the coil at the top left corner and exits it at the bottom left following a boustrophedon path, the black triangles pointing in the direction of the flow, whilst the numbers indicate the temperature in degrees Celsius, which is plotted once every ten elements. It is clear how the fluid exits with modest subcooling (around two degrees). The plot is similar for all the cases, as the differences in total cooling power are reflected in the refrigerant flow rate through the condenser, in this case $\dot{m}_r = 1.33\,\mathrm{kg\,s^{-1}}$. Contour plots of specific enthalpy and temperature over the coil and in the fill-pack are other outputs of the code. An example is shown in Fig. 6 for the same combination of correlations as Fig. 5.

Starting from the top left and moving clockwise, plot (a) represents the specific enthalpy of air in the tube bundle, ($\mathrm{kJ\,kg^{-1}}$), plot (b) shows the water temperature, (°C), distribution over the cooling coil, plot (c) is the water temperature, (°C), in the fill pack and plot (d) is the enthalpy of dry air in the fill pack, ($\mathrm{kJ\,kg^{-1}}$). The white arrows describe the main flow direction of the fluids, i.e. air in the left column and water in the right one: it is evident how the two streams are in co-flow in the tube bundle and in cross-flow in the fill pack. One advantage of the distributed-parameter model over a lumped-parameter approach is that quantities like those in Fig. 6 can be appreciated in their spatial distribution, which highlights a pattern consistent with the physical behaviour which should be expected. Indeed the enthalpy isoclines, Fig. 6(a), are almost perpendicular to the main flow direction for air, owing to the constant temperature inside the tubes during condensation, with a slight bend upwards on the left side, where the superheated ammonia enters the tube bundle. The very same trend is exhibited by the water temperature, Fig. 6(b), possibly even more pronounced. It can also be seen how the average water temperature at the exit of the tube bundle (lower edge in Fig. 6(b)) differs from the same value at the entrance of the coil (upper edge of 6(b)), owing to the presence of the fill-pack, Fig. 6(c), which effectively cools the water some 2.5 K, thus demonstrating its usefulness. The trends of water temperature and specific enthalpy in the fill-pack, Fig. 6(c) and (d) are best examined together. Owing to the cross-flow arrangement, water starts to be cooled from the top left of the pack, increasing the enthalpy of air, which explains the slanted trend of the isoclines for both quantities: since the water cools flowing from top to bottom, the enthalpy of air increases more slowly at the bottom left.

The same family of plots, conversely, is also able to describe and explain the influence of an unsuitable combination in the correlations to determine convective transport coefficients. This is readily demonstrated in Fig. 7, where the transport coefficients for heat transfer in the coil and mass transfer in the fill-pack are computed through the correlation recommended by Dreyer, [11], and that for mass transfer in the tube bundle is calculated according to Mizushina,[33]. The trends are apparently similar to those of Fig. 6, yet significant differences can be highlighted. The specific enthalpy has a much lower increase in the latter case, $5\,\mathrm{kJ\,kg^{-1}}$ instead of $15\,\mathrm{kJ\,kg^{-1}}$, which indicates that mass transfer (which is responsible for the evaporative cooling) is low.

This is also true for the fill-pack, Fig. 7(d), which shows an enthalpy exchange of $9\,\mathrm{kJ\,kg^{-1}}$ instead of almost $20\,\mathrm{kJ\,kg^{-1}}$. The lower mass transfer influences also the form of the isoclines, which are far less slanted and tend to fan out at the bottom, when both fluid streams have come into contact long enough for transport phenomena to become more apparent. The temperature of water for the case of Fig. 7 has a lower increase (2.1 K) than for Fig. 6, and water enters the tube bundle at a higher temperature than for the former case (29.7 °C instead of 28.4 °C), a further indication of poor performance of the correlation

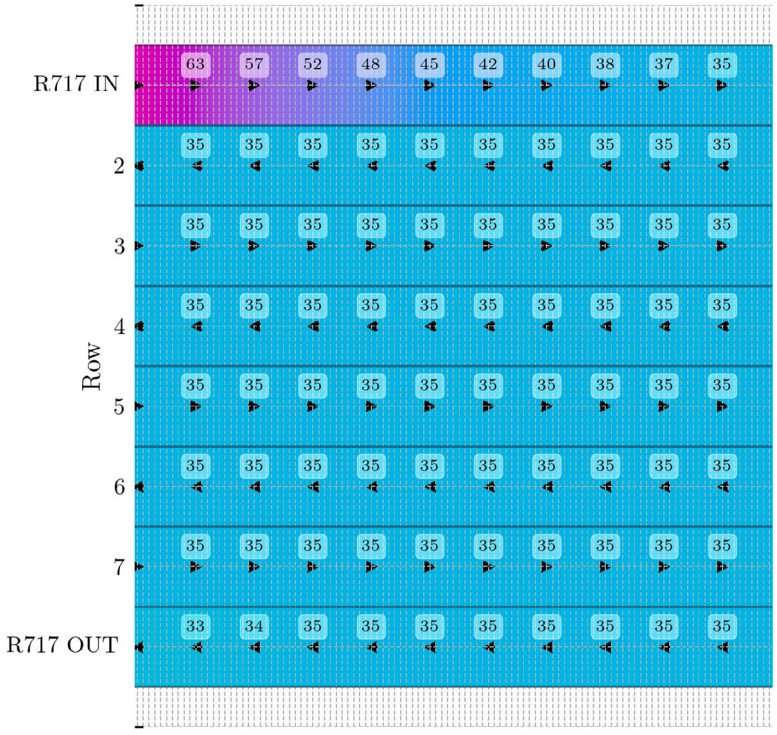

Fig. 5. Refrigerant temperature (°C) over the cooling coil is represented by a colour-map plot. The arrows indicate the flow direction, while the numbers on the left stay for the coils rows.

chosen for the fill-pack; indeed this combination is not among the top twenty represented in Fig. 8.

5.3. Integral evaluation of the condenser heat transfer rate

The code allows computation of integral (i.e. related to the evaporative condenser as a whole) quantities, among which the most significant are the cooling power, $\dot{Q}_r$, that is the heat transfer from the refrigerant to ambient, and its two components, namely the contribution due to convection $\dot{Q}_a$ and the one due to mass transfer (evaporation), $\dot{Q}_w$: this piece of information is the desired output for the model when employed in the simulation of a whole refrigeration plant. Also, the cooling power is the test quantity to verify which set of correlations comes closest to the reference value used for comparison, $\dot{Q}_0$.

The results of the tests for which $\dot{Q}_r$ falls within ±5% of $\dot{Q}_0$ are plotted in Fig. 8. Each bar represents the total heat transfer $\dot{Q}_r$, with the light blue stretch corresponding to $\dot{Q}_a$ and the blue one to $\dot{Q}_w$. The dotted lines represent the reference value, $\dot{Q}_0 = 1610\,\mathrm{kW}$, and the lower and upper bounds, ±5%. The correlation set used for the transport coefficients is reported for each bar on the y-axis, in the same order and with the same meaning as in Fig. 4, that is convective mass transfer in the coil, convective mass transfer in the fill-pack, convective heat transfer in the coil, and D for Dreyer, H for Hasan, M for Mizushina, N for Nitsu, P for Parker and Z for Zheng.

The ratio of convective to evaporative cooling is consistent with such pieces of equipment [4]. The plot demonstrates how several combinations – twenty in fact – yield results very close to the target value, and there seems to be no ground to state that correlations for all transport phenomena suggested by the same Authors should be chosen whenever possible, as recommended in [11,41].

5.4. Applicability of the coefficients

The correlations proved themselves robust enough to be employable out of the parameter range for which they were obtained: in fact, none of the combinations reported in Fig. 8 had all its parameters within the declared range of validity, still the results were more than satisfactory. When the maximum acceptable deviation from the target value is larger, the number of combinations increases further. Table 1 shows the 55 correlations which yield a result within ±10% of $\dot{Q}_0$; if the range of acceptance is increased to ±20% about 110 combinations satisfy the requirement. Interestingly, none of the correlations overestimates the total cooling power by more than 5%; this, in the Authors' opinion is due to the use of Shah's correlation for condensation, which might underestimate the heat transfer coefficient, contrary to the conclusions of Park and Hrnjak, [38].

To build more confidence on the results of the numerical tests performed, an ANOVA analysis has been carried out. The box plots in Fig. 9 are obtained comparing the rating heat rejection capacity to the values predicted by the model. The effect of the heat and mass coefficients both in the coil and in the fill-pack and the interface area coefficient are evaluated considering the deviation with respect to the rating performance. More details of the procedure can be found in [42], where a similar analysis is conducted for an evaporative condenser model developed according to the approach of Poppe. In general, the model tends to underestimate the heat rejection in all the tests performed; as said before, this could be related to the heat transfer coefficient for ammonia. Moreover, the parameters have different consequences on the model: Fig. 9(a) shows that the heat transfer coefficient has the strongest influence on the evaluation of the heat transfer rate and that Dreyer's correlation approximates the rating performance better; indeed all the top 20 combinations make use of it. On the other hand, the mass transfer coefficient both in the coil and in the fill pack seems to have less effect on the heat rejected by the refrigerant. In particular, four correlations for the mass transfer rate have similar outcomes, those of Zheng, Hasan, Parker and Nitsu; the correlation by Dryer for mass transfer rate causes the heat transfer rate to be underestimated even further, while that of Mizushima has in-between results. Finally, from this analysis emerges the also the interface area coefficient a_f has a negligible effect on the heat rejection compared with the other factors examined; so the selection of the coefficient proposed by Dreyer should be feasible as a tentative value in the absence of more precise estimations.

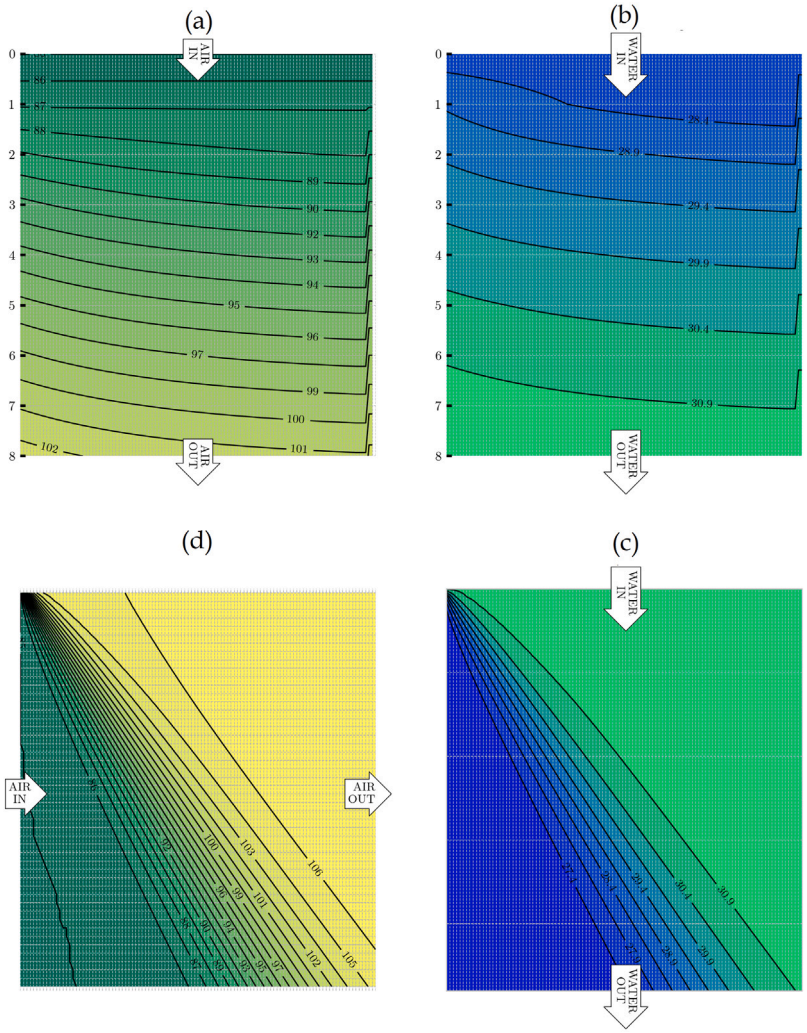

Fig. 6. Contour plots for specific enthalpy of air (J/kg) (a) and water temperature (°C) (b) in the cooling coil, and for specific enthalpy of air (J/kg) (c) and water temperature (°C) (d) in the fill pack. Set of correlations employed (N-Z-D): Nitsu for β_i, [34], Zheng for β_f, [23] and Dreyer for α_w, [36].

6. Conclusions

A distributed parameter, steady-state model of an evaporative condenser has been developed and successfully verified against the cooling capacity of a real-life piece of equipment. No model previously published in the open scientific literature dealt with the co-flow of water and air in the condenser coil. In the process, the model sensitivity to the choice of the correlations for the transport (heat and mass transfer) coefficients has been investigated to ascertain which combinations would yield the best results. It has been found that a comparatively large number - twenty - of combinations yield results within ±5% of the target value, which are thus likely to be within the experimental uncertainty of the manufacturer's data and can therefore be considered of equal accuracy. The analysis also pointed out that the number of combinations increases to 55 if a larger difference, ±10%, is accepted, jumping to 110 for a ±20% allowance.

The correlations proved robust enough to yield satisfactory results even when applied outside of the parameter range for which they were obtained and no evidence was found that using the same family, i.e. obtained by the same research group, of correlations for all transport coefficients would yield better results, contrary to what suggested by [11,41].

The peculiar structure of the model yields as outputs the spatial distribution of quantities such as specific enthalpy of air and water temperature for both the cooling coil and the fill-pack, and this piece of information can be used to highlight the reasons for the good or poor performance of the set of correlations chosen. The model has been developed to serve as a block of a larger system describing a refrigeration plant for food storage applications, and has been successfully employed in [3], but is fully self-contained and can therefore be used for design purposes or readily expanded to account for transient operations.

CRediT authorship contribution statement

M. Giovannini: Writing – original draft, Visualization, Validation, Supervision, Software, Resources, Methodology, Investigation, Formal analysis, Data curation, Conceptualization. **M. Lorenzini:** Writing – review & editing, Visualization, Validation, Supervision, Resources, Project administration, Methodology, Investigation, Funding acquisition, Formal analysis, Data curation, Conceptualization.

Declaration of competing interest

The authors declare that they have no known competing financial interests or personal relationships that could have appeared to influence the work reported in this paper.

Data availability

Data will be made available on request.

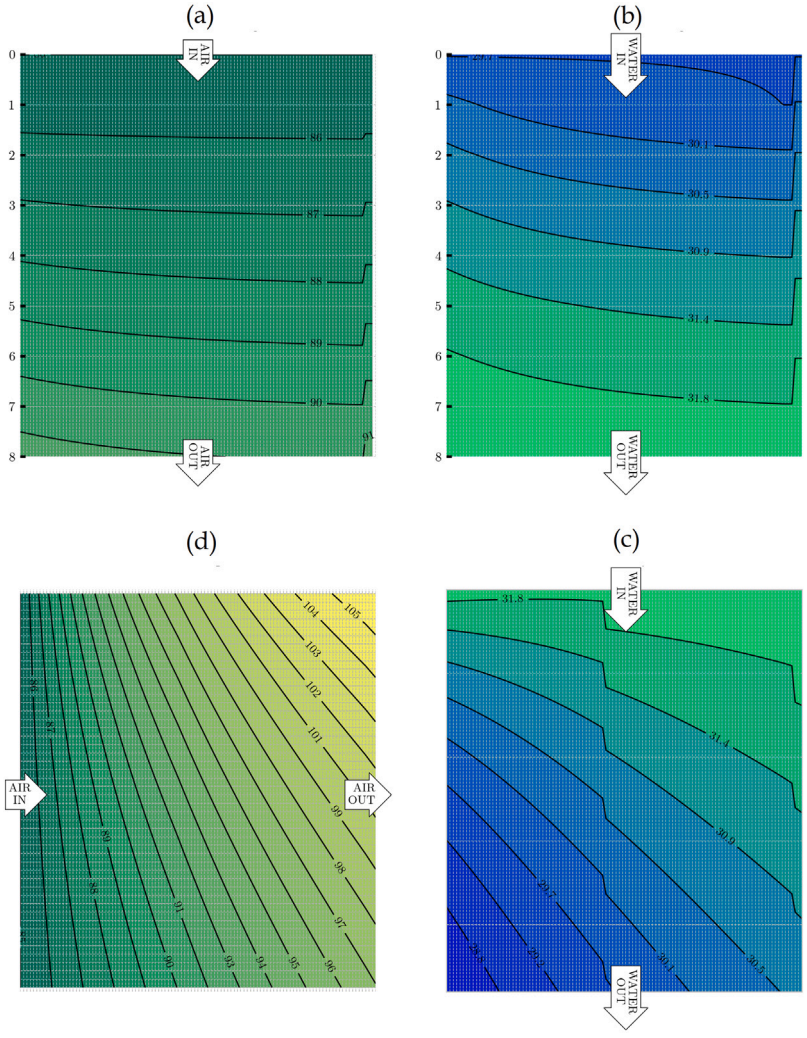

Fig. 7. Contour plots for specific enthalpy of air (J/kg) (a) and water temperature (°C) (b) in the cooling coil, and for specific enthalpy of air (J/kg) (c) and water temperature (°C) (d) in the fill pack. Set of correlations employed (M-D-D): Mizushina for β_t, [33], Dreyer for β_f, [36] and Dreyer for α_w, [36].

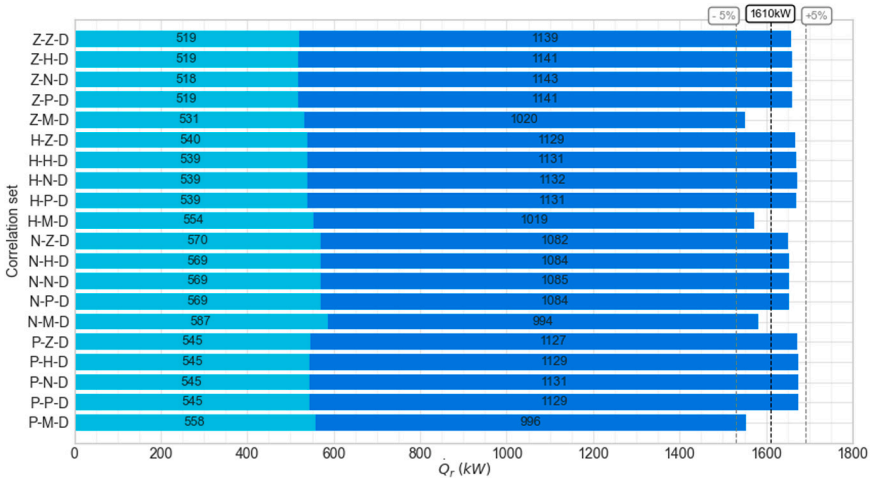

Fig. 8. Heat transfer to air (light blue) and water (blue) for the sets of correlations yielding a total cooling power $\dot{Q}_r$ within ±5% of $\dot{Q}_0$, (1610 kW); On the left the combination in the following order: mass transfer in the coil, convective mass transfer in the fill-pack and convective heat transfer in the coil. The letter stays D for Dreyer, H for Hasan, M for Mizushina, *N* for Nitsu, P for Parker and Z for Zheng.

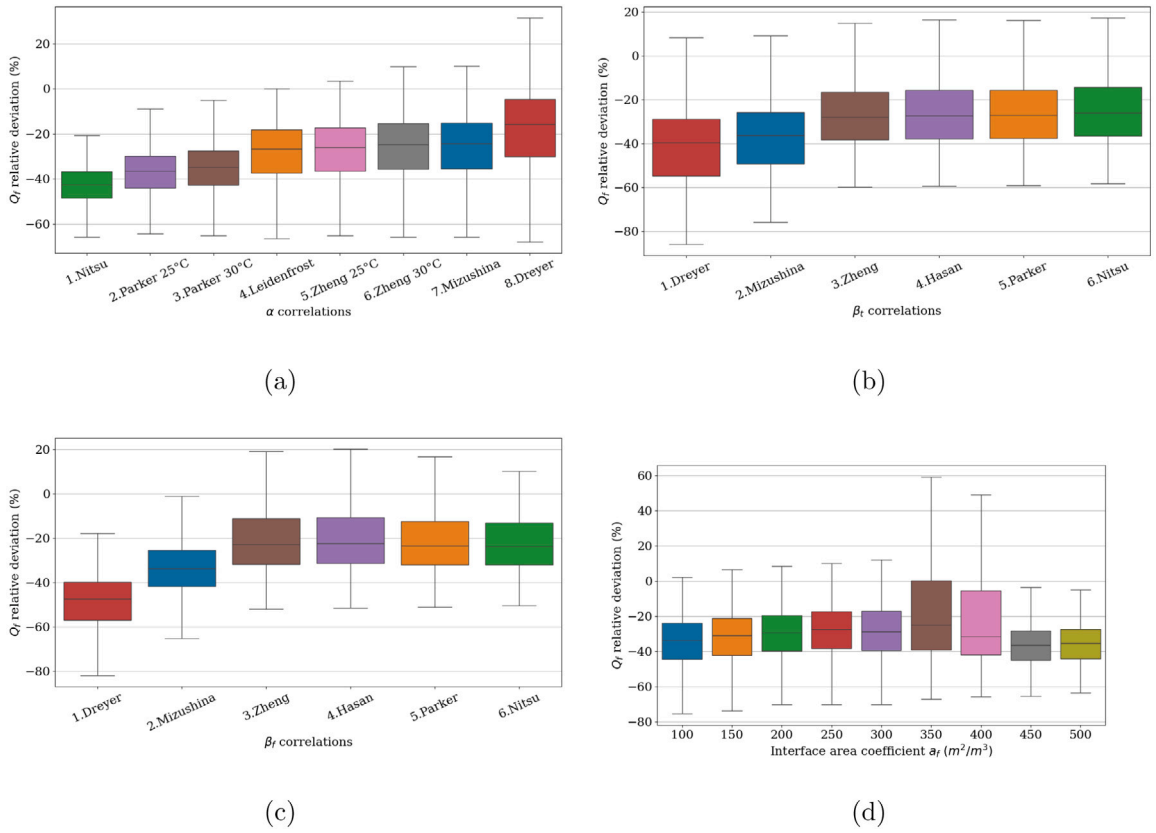

Fig. 9. Anova analysis of evaporative model according to Merkel approach. The effect of the heat transfer coefficient in the coil (a), the mass transfer coefficient in the coil (b) and in the fill-pack (c), and the interface area coefficient (d) are investigated.

Table 1
Set of correlations yielding results within ±10% of $\dot{Q}_0$.

β_t –	β_f –	α –	$\dot{m}$ kg s^{-1}	$\dot{Q}_a$ kW	$\dot{Q}_w$ kW	$\dot{Q}_r$ kW
Parker	Nitsu	Dreyer	1.36	545	1131	1675
Parker	Parker	Dreyer	1.36	545	1129	1674
Parker	Hasan	Dreyer	1.36	545	1129	1674
Parker	Zheng	Dreyer	1.36	545	1127	1672
Hasan	Nitsu	Dreyer	1.36	539	1132	1671
Hasan	Parker	Dreyer	1.36	539	1131	1670
Hasan	Hasan	Dreyer	1.36	539	1131	1670
Hasan	Zheng	Dreyer	1.36	540	1129	1668
Zheng	Nitsu	Dreyer	1.36	518	1143	1661
Zheng	Parker	Dreyer	1.36	519	1141	1660
Zheng	Hasan	Dreyer	1.36	519	1141	1660
Zheng	Zheng	Dreyer	1.36	519	1139	1658
Nitsu	Nitsu	Dreyer	1.34	569	1085	1654
Nitsu	Parker	Dreyer	1.34	569	1084	1653
Nitsu	Hasan	Dreyer	1.34	569	1084	1653
Nitsu	Zheng	Dreyer	1.33	570	1082	1651
Nitsu	Mizushina	Dreyer	1.28	587	994	1581
Hasan	Mizushina	Dreyer	1.27	554	1019	1573
Parker	Mizushina	Dreyer	1.26	558	996	1554
Zheng	Mizushina	Dreyer	1.25	531	1020	1551
Nitsu	Nitsu	Mizushina	1.22	502	990	1492
Nitsu	Parker	Mizushina	1.21	502	989	1491
Nitsu	Hasan	Mizushina	1.21	503	989	1491
Nitsu	Zheng	Mizushina	1.21	503	987	1490
Nitsu	Nitsu	Zheng 30 °C	1.21	501	986	1488
Nitsu	Parker	Zheng 30 °C	1.21	502	986	1487
Nitsu	Hasan	Zheng 30 °C	1.21	502	985	1487
Nitsu	Zheng	Zheng 30 °C	1.21	502	984	1486
Parker	Nitsu	Mizushina	1.20	477	999	1475
Parker	Parker	Mizushina	1.20	477	998	1475
Parker	Hasan	Mizushina	1.20	477	998	1475
Parker	Zheng	Mizushina	1.20	477	996	1474
Hasan	Nitsu	Mizushina	1.19	471	998	1469
Hasan	Parker	Mizushina	1.19	471	997	1468
Hasan	Hasan	Mizushina	1.19	471	997	1468
Parker	Nitsu	Zheng 30 °C	1.19	474	993	1468
Hasan	Nitsu	Zheng 30 °C	1.19	470	997	1468
Parker	Parker	Zheng 30 °C	1.19	475	992	1467
Parker	Hasan	Zheng 30 °C	1.19	475	992	1467
Hasan	Zheng	Mizushina	1.19	472	995	1467
Parker	Zheng	Zheng 30 °C	1.19	475	991	1466
Hasan	Parker	Zheng 30 °C	1.19	470	995	1465
Hasan	Hasan	Zheng 30 °C	1.19	470	995	1465
Hasan	Zheng	Zheng 30 °C	1.19	470	994	1464
Zheng	Nitsu	Mizushina	1.19	453	1007	1460
Zheng	Parker	Mizushina	1.19	453	1007	1459
Zheng	Hasan	Mizushina	1.19	453	1006	1459
Zheng	Nitsu	Zheng 30 °C	1.20	453	1006	1459
Zheng	Zheng	Mizushina	1.19	453	1005	1458
Zheng	Parker	Zheng 30 °C	1.20	453	1005	1458
Zheng	Hasan	Zheng 30 °C	1.20	454	1005	1458
Zheng	Zheng	Zheng 30 °C	1.20	454	1003	1457
Nitsu	Nitsu	Zheng 25 °C	1.19	490	964	1454
Nitsu	Parker	Zheng 25 °C	1.19	490	963	1454
Nitsu	Hasan	Zheng 25 °C	1.19	490	963	1453
Nitsu	Zheng	Zheng 25 °C	1.19	491	962	1453

References

[1] G. Ribatski, A.M. Jacobi, Falling-film evaporation on horizontal tubes—a critical review, Int. J. Refrig. 28 (5) (2005) 635–653, http://dx.doi.org/10.1016/j.ijrefrig.2004.12.002.

[2] K. Harby, D.R. Gebaly, N.S. Koura, M.S. Hassan, Performance improvement of vapor compression cooling systems using evaporative condenser: An overview, Renew. Sustain. Energy Rev. 58 (2016) 347–360, http://dx.doi.org/10.1016/j.rser.2015.12.313, URL: https://www.sciencedirect.com/science/article/pii/S1364032115016962.

[3] M. Giovannini, M. Lorenzini, Numerical model of an industrial refrigeration system for condensation temperature optimisation, Therm. Sci. Eng. Prog. 42 (2023) http://dx.doi.org/10.1016/j.tsep.2023.101846.

[4] V. Lebedev, Refrigerating Engineering, MIR, Moscow, 1986.

[5] E. Bonauguri, D. Miari, Tecnica del Freddo, Hoepli, Milan, 1988, (in Italian).

[6] BAC, Baltimore aircoil company, 2024, URL: https://www.baltimoreaircoil.eu/it/prodotti/CXVE, (Accessed 22 April 2024).

[7] M.H. Zaidan, F.M. Abed, A.T. Derea, Performance improving the compression cooling system by adding a cooling pad on the condenser, AIP Conf. Proc. 2787 (1) (2023) 030013, http://dx.doi.org/10.1063/5.0149025.

[8] F. Merkel, Verdunstungskühlung, VDI-Zeitchrift 70 (1925) 123–128.

[9] M. Poppe, H. Rögener, Berechnung von Rückkühlwerken, VDIWärmeatlas (1991) Mi 1–Mi 15.

[10] D.R. Baker, H.A. Shryock, A comprehensive approach to the analysis of cooling tower performance, J. Heat Transfer 83 (3) (1961) 339–349, http://dx.doi.org/10.1115/1.3682276.

[11] A.A. Dreyer, Analysis of Evaporative Coolers and Condensers (Ph.D. thesis), Stellenbosch University, Stellenbosch, 1988.

[12] A.A. Dreyer, P.J. Erens, Modelling of cooling tower splash pack, Int. J. Heat Mass Transfer 39 (1) (1996) 109–123, http://dx.doi.org/10.1016/S0017-9310(96)85010-1.

[13] W. Zalewski, Mathematical model of heat and mass transfer processes in evaporative condensers, Int. J. Refrig. 16 (1) (1993) 23–30, http://dx.doi.org/10.1016/0140-7007(93)90017-3.

[14] W. Zalewski, P.A. Gryglaszewski, Mathematical model of heat and mass transfer processes in evaporative fluid coolers, Chem. Eng. Process.: Process Intensif. 36 (4) (1997) 271–280, http://dx.doi.org/10.1016/S0255-2701(97)00006-8.

[15] B. Halasz, A general mathematical model of evaporative cooling devices, Rev. Gén. Therm. 37 (4) (1998) 245–255, http://dx.doi.org/10.1016/S0035-3159(98)80092-5.

[16] A. Hasan, K. Sirén, Theoretical and computational analysis of closed wet cooling towers and its applications in cooling of buildings, Energy Build. 34 (5) (2002) 477–486, http://dx.doi.org/10.1016/S0378-7788(01)00131-1.

[17] A.A. Hasan, Performance Analysis of Heat Transfer Process from Wet and Dry Surfaces: Cooling Towers and Heat Exchangers Report A10 (Ph.D. thesis), Helsinki University of Technology, 2005.

[18] D.G. Kröger, Air-Cooled Heat Exchangers and Cooling Towers, vol. 1, PennWell Books, 2004.

[19] J.C. Kloppers, D.G. Kröger, The Lewis factor and its influence on the performance prediction of wet-cooling towers, Int. J. Therm. Sci. 44 (9) (2005) 879–884, http://dx.doi.org/10.1016/j.ijthermalsci.2005.03.006.

[20] B.A. Qureshi, S.M. Zubair, A comprehensive design and rating study of evaporative coolers and condensers. Part I. Performance evaluation, Int. J. Refrig. 29 (4) (2006) 645–658, http://dx.doi.org/10.1016/j.ijrefrig.2005.09.014.

[21] J. Facao, A.C. Oliveira, Heat and mass transfer in an indirect contact cooling tower: CFD simulation and experiment, Numer. Heat Transfer A 54 (10) (2008) 933–944.

[22] A. Yilmaz, Analytical calculation of wet cooling tower performance with large cooling ranges, J. Therm. Sci. Technol. 30 (2) (2010) 45–56.

[23] W.-Y. Zheng, D.-S. Zhu, J. Song, L.-D. Zeng, H.-j. Zhou, Experimental and computational analysis of thermal performance of the oval tube closed wet cooling tower, Appl. Therm. Eng. 35 (2012) 233–239, http://dx.doi.org/10.1016/j.applthermaleng.2011.10.047.

[24] W.-Y. Zheng, D.-S. Zhu, G.-Y. Zhou, J.-F. Wu, Y.-Y. Shi, Thermal performance analysis of closed wet cooling towers under both unsaturated and supersaturated conditions, Int. J. Heat Mass Transfer 55 (25) (2012) 7803–7811, http://dx.doi.org/10.1016/j.ijheatmasstransfer.2012.08.006.

[25] O.M. Hernández-Calderón, E. Rubio-Castro, E.Y. Rios-Iribe, Solving the heat and mass transfer equations for an evaporative cooling tower through an orthogonal collocation method, Comput. Chem. Eng. 71 (2014) 24–38, http://dx.doi.org/10.1016/j.compchemeng.2014.06.008.

[26] J.R. Ortiz-del-Castillo, O.M. Hernández-Calderón, E.Y. Rios-Iribe, M.D. González-Llanes, E. Rubio-Castro, M.E. Cervantes-Gaxiola, Analytical solution of the governing equations for heat and mass transfer in evaporative cooling process, Int. J. Refrig. 111 (2020) 178–187, http://dx.doi.org/10.1016/j.ijrefrig.2019.11.019.

[27] J. du Plessis, M. Owen, A validated discretized thermal model for application in bare tube evaporative coolers and condensers, Appl. Therm. Eng. 175 (2020) 115407, http://dx.doi.org/10.1016/j.applthermaleng.2020.115407.

[28] V.W. Bhatkar, Experimental study of multistage indirect evaporative coolers, JP J. Heat Mass Transf. 24 (3) (2021) 69–77, http://dx.doi.org/10.17654/HM0240100069.

[29] Y. Li, S. Shen, Z. Li, C. Wang, Z. Xing, D. Ren, H. Zhang, Mathematical model of the evaporative condenser for on-site condition simulation, Int. J. Refrig. 162 (2024) 121–131, http://dx.doi.org/10.1016/j.ijrefrig.2024.03.017, URL: https://www.sciencedirect.com/science/article/pii/S0140700724001208.

[30] M.K. Mansour, Practical effectiveness-NTU model for cooling and dehumidifying coil with non-unit Lewis Factor, Appl. Therm. Eng. 100 (2016) 1111–1118, http://dx.doi.org/10.1016/j.applthermaleng.2016.02.096.

[31] I.H. Bell, J. Wronski, S. Quoilin, V. Lemort, Pure and pseudo-pure fluid thermophysical property evaluation and the open-source thermophysical property library CoolProp, Ind. Eng. Chem. Res. 53 (6) (2014) 2498–2508, http://dx.doi.org/10.1021/ie4033999, URL: http://pubs.acs.org/doi/abs/10.1021/ie4033999. arXiv:http://pubs.acs.org/doi/pdf/10.1021/ie4033999.

[32] R. Parker, R. Treybal, The heat mass transfer characteristics of evaporative coolers, Chem. Eng. Prog. Symp. Ser. 57 (32) (1961) 138–149.
[33] T. Mizushina, R. Ito, H. Miyashita, Experimental study of an evaporative cooler, Int. Chem. Eng. 7 (4) (1967) 727–732, Cited By :83.
[34] Y. Niitsu, K. Naito, T. Anzai, Studies on characteristics and design procedure of evaporative coolers, J. SHASE Jpn. 43 (7) (1969) 581–590.
[35] W. Leidenfrost, B. Korenic, Analysis of evaporative cooling and enhancement of condenser efficiency and of coefficient of performance, Wärme- Stoffübertrag. 12 (1) (1979) 5–23, http://dx.doi.org/10.1007/BF01672437.
[36] P.J. Erens, A.A. Dreyer, A general approach for the rating of evaporative closed circuit coolers, 1989, p. 11.
[37] H.B. Komandiwirya, P.S. Hrnjak, T.A. Newell, An experimental investigation of pressure drop and heat transfer in an in-tube condensation system of ammonia with and without miscible oil in smooth and enhanced tubes, 2005.
[38] C.Y. Park, P. Hrnjak, NH3 in-tube condensation heat transfer and pressure drop in a smooth tube, Int. J. Refrig. 31 (4) (2008) 643–651, http://dx.doi.org/10.1016/j.ijrefrig.2008.01.005.
[39] M.M. Shah, A general correlation for heat transfer during film condensation inside pipes, Int. J. Heat Mass Transfer 22 (4) (1979) 547–556, http://dx.doi.org/10.1016/0017-9310(79)90058-9.
[40] J.M. Wu, X. Huang, H. Zhang, Numerical investigation on the heat and mass transfer in a direct evaporative cooler, Appl. Therm. Eng. 29 (1) (2009) 195–201, http://dx.doi.org/10.1016/j.applthermaleng.2008.02.018.
[41] I.C. Finlay, W. Grant, The Accuracy of Some Simple Methods of Rating Evaporative Coolers, National Engineering Laboratory, Department of Trade and Industry, 1974.
[42] M. Giovannini, M. Lorenzini, Analysis of variance of the heat and mass transfer coefficients in an evaporative condenser, J. Phys. Conf. Ser. 2509 (1) (2023) 012018, http://dx.doi.org/10.1088/1742-6596/2509/1/012018, Publisher: IOP Publishing.